ChemPubSoc Europe

DOI: 10.1002/ejic.201501336

EurJIC European Journal of Inorganic Chemistry

Full Paper

Anticancer Complexes

Synthesis, Characterization, Reactivity, Catalytic Activity, and Antiamoebic Activity of Vanadium(V) Complexes of ICL670 (Deferasirox) and a Related Ligand

Mannar R. Maurya,*[a] Bithika Sarkar,[a] Fernando Avecilla,[b] Saba Tariq,[c] Amir Azam,[c] and Isabel Correia[d]

Abstract: The reactions of $[V^{IV}O(acac)_2]$ (acac = acetylacetonato) with two ONO tridentate ligands, 4-[3,5-bis(2-hydroxyphenyl)-1,2,4-triazol-1-yl]benzoic acid (H_2L^1, **I**) and 3,5-bis(2-hydroxyphenyl)-1-phenyl-1,2,4-triazole (H_2L^2, **II**) in methanol lead to the formation of the oxidovanadium(V) complexes $[V^VO(\mu\text{-}L^1)(OMe)]_2$ (**1**) and $[V^VO(\mu\text{-}L^2)(OMe)]_2$ (**2**). In the presence of KOH/CsOH, they give the corresponding dioxidovanadium(V) complexes. The isolated complexes $K(H_2O)[V^VO_2(L^1)]$ (**3**), $K(H_2O)[V^VO_2(L^2)]$ (**4**), $Cs(H_2O)[V^VO_2(L^1)]$ (**5**), and $Cs(H_2O)[V^VO_2(L^2)]$ (**6**) along with **1** and **2** have been characterized by various spectroscopic techniques (FTIR; UV/Vis; ^1H, ^{13}C, and ^{51}V NMR), elemental analysis, thermal studies, MALDI-TOF MS analysis, and single-crystal analysis of **1a** (complex **1** grown together with 4,4′-bipyridyl). The oxidative bromination of thymol, catalyzed by these complexes, in the presence of KBr and $HClO_4$ with H_2O_2 as an oxidant, gives 2-bromothymol, 4-bromothymol, and 2,4-dibromothymol. The amounts of the catalyst, oxidant, KBr, $HClO_4$, and the solvent were optimized for the maximum conversion of thymol. Both ligands and all complexes were tested in vitro for antiamoebic activity against the HM1:IMSS strain of *Entamoeba histolytica* by a microdilution method. The complexes are more potent amoebicidal agents than the standard drug metronidazole. Toxicity studies against a human cervical cancer cell line (HeLa) also confirm that these compounds are less cytotoxic than metronidazole.

Introduction

4-[3,5-Bis(2-hydroxyphenyl)-1,2,4-triazol-1-yl]benzoic acid (ICL670), commonly known as deferasirox, is a promising drug approved for the oral treatment of transfusional iron overload in patients suffering from chronic anemia, including β-thalassemia.[1] The complexing behavior of deferasirox and related ligands towards Fe^{II} and Fe^{III} ions, their stability, redox properties, and catalytic potential for Fenton reactions in biological media have been investigated recently.[2]

The dibasic tridentate ONO functionalities of deferasirox and related ligands with a triazole group have high potential for the design of structural models of vanadate-dependent haloperoxidase enzymes (VHPOs).[3,4] Structural models of VHPOs and their use as functional mimics have attracted the attention of researchers and found tremendous growth over the past few years.[5–8] In VHPOs, the vanadium centers bind covalently to the N_ε atoms of imidazole rings in the active sites of enzymes.[9,10] Therefore, we have selected 4-[3,5-bis(2-hydroxyphenyl)-1,2,4-triazol-1-yl]benzoic acid (ICL670, H_2L^1), and 3,5-bis(2-hydroxyphenyl)-1-phenyl-1,2,4-triazole (H_2L^2, Scheme 1) and prepared their vanadium(V) complexes. The obtained complexes are able to model the structural features of VHPOs and are also functional models, owing to their catalytic activity in the oxidative bromination of thymol by H_2O_2.

Another relevant field based on vanadium chemistry is the biological/medicinal potential of vanadium compounds.[11] Their antiamoebic activity against *Entamoeba histolytica*[12] and antitrypanosomal activity against *Trypanosoma cruzi*[13] have been established in addition to other therapeutic applications.[11] *E. histolytica*, an aerobic parasitic protozoan, causes life-threatening amoebiasis, a contagious disease of the human gastrointestinal tract. According to the World Health Organization, this disease causes approximately 110000 deaths and affects almost 500 million people annually.[14,15] In amoebiasis, the protozoan affects all body organs, destroys human tissue, and leads to diseases such as hemorrhagic colitis and extra intestinal abscesses.[16] The most effective drug for amoebiasis is metronidazole (MNZ).[17] However, in the last two decades, it has been reported that MNZ is mutagenic towards bacteria, causes tumors in rodents, and presents toxic effects such as genotoxicity, gastric mucus irritation, and spermatoid damage.[18] Therefore, new, effective antiamoebic agents that have greater potency and efficacy with lower toxicity are required.

[a] *Department of Chemistry, Indian Institute of Technology Roorkee, Roorkee 247667, India*
E-mail: rkmanfcy@iitr.ac.in
www.iitr.ac.in/~CY/rkmanfcy
[b] *Department of Chemistry, Jamia Millia Islamia, Jamia Nagar, New Delhi 100025, India*
[c] *Departamento de Química Fundamental, Universidade da Coruña, Campus de A Zapateira, 15071 A Coruña, Spain*
[d] *Centro de Química Estrutural, Instituto Superior Técnico, Universidade de Lisboa, Av. Rovisco Pais 1, 1049-001 Lisbon, Portugal*

Supporting information and ORCID(s) from the author(s) for this article are available on the WWW under http://dx.doi.org/10.1002/ejic.201501336.

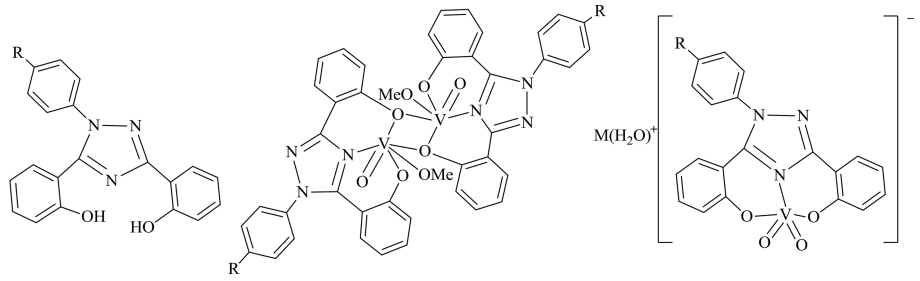

R	Ligand	Complex
COOH	H_2L^1	$[VO(\mu\text{–}L^1)(OMe)]_2$ (**1**)
H	H_2L^2	$[VO(\mu\text{–}L^2)(OMe)]_2$ (**2**)

M	R	Complex
K	COOH	$K(H_2O)[VO_2(L^1)]$ (**3**)
K	H	$K(H_2O)[VO_2(L^2)]$ (**4**)
Cs	COOH	$Cs(H_2O)[VO_2(L^1)]$ (**5**)
Cs	H	$Cs(H_2O)[VO_2(L^2)]$ (**6**)

Scheme 1. Overview of the ligands and complexes described in this work.

In recent decades, there has been a remarkable growth in research into the synthesis of nitrogen-containing heterocyclic derivatives. Ring systems containing 1,2,4-triazoles have attracted considerable scientific interest because of their varied chemical properties, synthetic versatility, and pharmacological activities, such as antibacterial,[19] antifungal[20] antitubercular,[21] anti-inflammatory,[22] anticancer,[23] anticonvulsant,[24] antiviral,[25] and antidepressant[26] properties. Several drugs in the market contain the 1,2,4-triazole moiety, for example, astriazolam[27] and etizolam.[28] The promising antiamoebic activity of the 1,2,4-triazole scaffold has also been reported recently.[29] For these reasons and to further explore the biological activity of vanadium complexes, we studied the antiamoebic and cytotoxic activity of monooxidovanadium(V) and dioxidovanadium(V) complexes of H_2L^1 and H_2L^2, and the results are reported herein.

Results and Discussion

The reactions of $[V^{IV}O(acac)_2]$ (acac = acetylacetonato) with H_2L^1 (**I**) and H_2L^1 (**II**) in 1:1 molar ratios in methanol under reflux followed by aerial oxidation yield the dinuclear oxidovanadium(V) complexes $[V^VO(\mu\text{-}L^1)(OMe)]_2$ (**1**) and $[V^VO(\mu\text{-}L^2)(OMe)]_2$ (**2**), respectively. The dropwise addition of a methanolic solution of KOH or CsOH to a methanol solution of these complexes gradually leads to the formation of the corresponding V^VO_2 complexes $K(H_2O)[V^VO_2(L^1)]$ (**3**) and $K(H_2O)[V^VO_2(L^2)]$ (**4**) or $Cs(H_2O)[V^VO_2(L^1)]$ (**5**) and $Cs(H_2O)[V^VO_2(L^2)]$ (**6**). The synthetic procedures are summarized in Equations (1), (2), and (3) for H_2L^1 as the representative ligand.

$$2[V^{IV}O(acac)_2] + 2H_2L^1 + 2MeOH + 1/2O_2 \rightarrow 2[V^VO(\mu\text{-}L^1)(OMe)]_2 + 4Hacac + H_2O \quad (1)$$

$$[V^VO(\mu\text{-}L^1)(OMe)]_2 + 2KOH + 2H_2O \rightarrow 2K(H_2O)[V^VO_2(L^1)] + 2MeOH \quad (2)$$

$$[V^VO(\mu\text{-}L^1)(OMe)]_2 + 2CsOH + 2H_2O \rightarrow 2Cs(H_2O)[V^VO_2(L^1)] + 2MeOH \quad (3)$$

Efforts to prepare a dinuclear complex connected through the two distinct mononuclear units present in **1** were unsuccessful. Complex **1** instead crystallized as $[V^VO(\mu\text{-}L^1)(OMe)]_2$·4,4′-bipy (**1a**, 4,4′-bipy = 4,4′-bipyridine), in which a 4,4′-bipy molecule is weakly associated with **1**. All of the complexes are soluble in *N*,*N*-dimethylformamide (DMF) and dimethyl sulfoxide (DMSO) and partially soluble in methanol and acetonitrile. The structures of the complexes described in this work are presented in Scheme 1 along with ligands. The structural formula of each complex is based on elemental analysis, thermal, and spectroscopic (IR; UV/Vis; ^1H, ^{13}C, and ^{51}V NMR) data as well as single-crystal X-ray analysis for **1a**.

Thermal Analysis

The thermal stability of the monomeric complexes **3**, **4**, **5**, and **6** was studied under an oxygen atmosphere. The complexes lose mass above 110 °C that is roughly equal to one water molecule indicating the presence of weekly coordinated water. As the temperature increases further, complex **3** decomposes exothermically in one step, whereas the others (**4**, **5**, and **6**) take two or three overlapping steps and form MVO_3 (M = K or Cs) as the final product. Complexes **1** and **2** are relatively more stable (up to ca. 310 °C) and only exhibit partial mass loss. A further increment in temperature leads to their decomposition to form V_2O_5 at ca. 400 °C. Further details of this study are presented in Table S1 and Figures S1 and S2 in the Supporting Information.

MALDI-TOF MS Analysis

MALDI-TOF MS analysis was performed to ascertain the existence of the proposed dimeric species of **1** and **2**. The MALDI-TOF MS analysis showed molecular ion peaks at *m*/*z* = 876.15 (calcd. 876.06) and 788.12 (calcd. 788.08) for **1** and **2** (Figures S3 and S4), respectively. These peaks are generated after the elimination of two weakly coordinated OMe groups from the metal centers in **1** and **2**.

Crystal Structure of $[V^VO(\mu\text{–}L^1)(OMe)]_2$·4,4′-bipy (1a)

Compound **1a** crystallized from methanol as black blocks, and an ORTEP representation is depicted in Figure 1. The asymmetric unit of **1a** contains half of the dinuclear complex and half a

4,4′-bipy molecule. Selected bond lengths and angles are listed in Table 1.

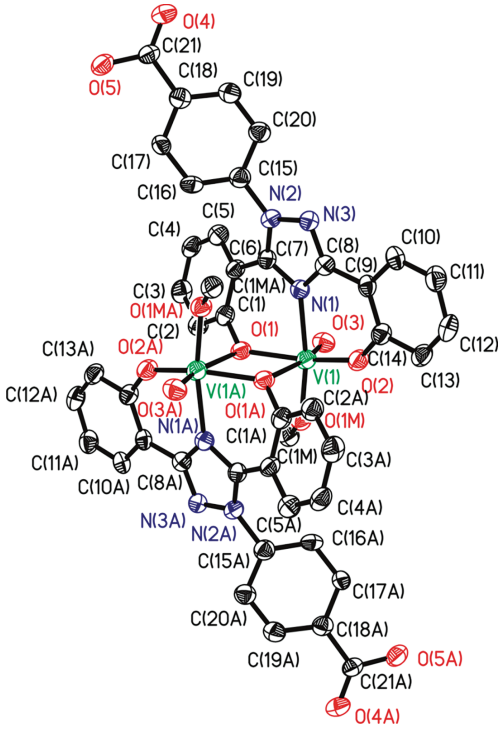

Figure 1. ORTEP plot of **1a** (CCDC-1437168). All non-hydrogen atoms are represented by 50 % probability ellipsoids. Hydrogen atoms and 4,4′-bipy molecule are omitted for clarity. Symmetry transformation used to generate equivalent atoms: #1 $-x + 1, -y + 1, -z + 1$.

Table 1. Bond lengths [Å] and angles [°] for **1a**.[a]

Bond	**1a**
V(1)–O(1)	1.924(4)
V(1)–O(1M)	1.790(4)
V(1)–O(2)	1.825(4)
V(1)–O(3)	1.593(4)
V(1)–N(1)	2.118(4)
V(1)–O(1)#1	2.409(4)
Angle	**1a**
O(3)–V(1)–O(1M)	99.40(18)
O(3)–V(1)–O(2)	105.8(2)
O(1M)–V(1)–O(2)	100.00(17)
O(3)–V(1)–O(1)	97.91(18)
O(1M)–V(1)–O(1)	91.39(16)
O(2)–V(1)–O(1)	151.49(18)
O(3)–V(1)–N(1)	92.23(18)
O(1M)–V(1)–N(1)	166.91(17)
O(2)–V(1)–N(1)	82.41(17)
O(1)–V(1)–N(1)	81.02(16)
O(3)–V(1)–O(1)#1	169.31(17)
O(1M)–V(1)–O(1)#1	84.08(15)
O(2)–V(1)–O(1)#1	83.41(16)
O(1)–V(1)–O(1)#1	71.79(16)
N(1)–V(1)–O(1)#1	83.43(15)

[a] Symmetry transformation used to generate equivalent atoms: #1 $-x + 1, -y + 1, -z + 1$.

The structure of **1a** contains one dinuclear complex grown by a symmetry operation, consisting of a tridentate ONO ligand (L^1) in a $[V^VO(\mu\text{-}OMe)_2V^VO]$ unit with an anti-coplanar configuration.[30] Each vanadium center is six-coordinate in a distorted octahedral geometry: ligand L^1 is bound through the triazole N atom [V1–N1 2.118(4) Å] and the two phenolic O atoms, one of which acts as a terminal ligand [V1–O2, 1.825(4) Å] and the other acts as a bridge [V1–O1 1.924(4) Å]; one terminal oxygen atom [V1–O3 1.593(4) Å] and one methoxy O atom [V1–O1M 1.790(4) Å] complete the coordination sphere. The V–μ-$O_{phenolate}$ bonds *trans* to the oxido groups are significantly longer [V1–O1#1 2.409(4) Å] than the others. The triazole group (C7, C8, N1, N2, N3) and one of the phenolate rings (C9, C10, C11, C12, C13, C14, O2) are coplanar [mean deviation from plane 0.0288(44) Å], and the other phenolate ring (C1, C2, C3, C4, C5, C6, O1), which acts as a bridge, forms a torsion angle of 26.98(17)° with the previous one. The vanadium atom is displaced towards the apical oxido ligand from the equatorial plane defined by the two $O_{phenolate}$, one $N_{triazole}$, and $O_{methoxy}$ atoms by 0.3001(19) Å [mean deviation from plane O1M–O2–N1–O1, 0.0976(19) Å]. The V=O bond is characteristic of oxido-type O atoms with strong π bonding.[31] The V–V separation of 3.521(19) Å is similar to those reported for other compounds.[32]

Intermolecular hydrogen bonds exit between the protonated $O_{carboxyl}$ and $N_{4,4'\text{-bipy}}$ atoms along the structure (see Table 2). These hydrogen bonds determine the molecular structure in which alternate 4,4′-bipy groups and dinuclear complexes form chains. The chains are packed as sandwich structures between 4,4′-bipy groups and dinuclear complexes, which are in contact through CH–π and van der Waals interactions (Figure 2).

Table 2. Hydrogen bonds in the **1a**.[a]

D–H···A	*d*(D–H)	*d*(H···A)	*d*(D···A)	<(DHA)
O(5)–H(5O)···N(4)#3	1.00	1.67	2.658(6)	167.7

[a] Symmetry transformation used to generate equivalent atoms: #3 $-x + 2, -y, -z$.

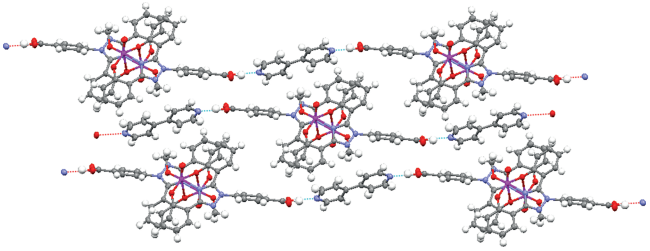

Figure 2. Crystal packing of **1a**. The hydrogen bonds that are shown in dashed blue lines form the chains. The sandwich structures formed by two 4,4′-bipy groups and one dinuclear complex can be seen in the center of the image.

IR Spectroscopy Study

A partial list of IR spectroscopic data of the ligands and complexes is presented in Table 3. Two strong bands at $\tilde{\nu}$ = 1618 and 912 cm^{-1} for **I** and at $\tilde{\nu}$ = 1624 and 938 cm^{-1} for **II** are assigned to ν(C=N) and ν(N–N) stretching, respectively. A bathochromic shift of ν(C=N) of 15–24 cm^{-1} in the spectra of all complexes indicates the coordination of the vanadium center through the nitrogen atom of the azomethine group. This is further supported by the shift of the ν(N–N) stretch to higher

wavenumbers, owing to reduced repulsion between the lone pairs of adjacent nitrogen atoms. The ν(C=O) band for the carboxylic acid in ligand **I** appears at $\tilde{\nu}$ = 1692 cm^{-1} and is slightly affected in the corresponding spectra of complexes. The broad band at $\tilde{\nu} \approx$ 3266 cm^{-1} might be assigned to ν(O–H) stretching owing to the presence of coordinated water. This band prevented the unequivocal identification of the coordination of the phenolic oxygen atom.

Table 3. IR spectroscopic data [cm^{-1}] of ligands and complexes.

	ν(–C=N–)	ν(–N–N–)	ν(V=O)/(VO_2)
H_2L^1 (**I**)	1618	912	–
H_2L^2 (**II**)	1624	938	–
$[V^VO(\mu\text{-}L^1)(OMe)]_2$ (**1**)	1605	1019	973
$[V^VO(\mu\text{-}L^2)(OMe)]_2$ (**2**)	1604	1022	968
$K(H_2O)[V^VO_2(L^1)]$ (**3**)	1605	1019	924/882
$K(H_2O)[V^VO_2(L^2)]$ (**4**)	1600	1029	936/923
$Cs(H_2O)[V^VO_2(L^1)]$ (**5**)	1603	1016	926/886
$Cs(H_2O)[V^VO_2(L^2)]$ (**6**)	1608	1026	930/905

The V^VO complexes **1** and **2** exhibit strong but relatively broad bands at $\tilde{\nu}$ = 973 and 970 cm^{-1}, respectively, for ν(V=O) stretching. The broadness of this band suggests a slight asymmetry in the dinuclear complexes. The presence of two such sharp bands in the spectra of the V^VO_2 complexes **3**–**6** in the $\tilde{\nu}$ = 882–936 cm^{-1} region for the ν_{sym}(O=V=O) and ν_{asym}(O=V=O) modes reinforces the assignment of a *cis*-[V^VO_2] structure in these complexes.[33]

Electronic Spectroscopy Study

The UV/Vis absorption spectra of the ligands exhibit three bands at λ = 205, 270, and 309 nm for **I** and at λ = 207, 239, and 304 nm for **II**, which are assigned to $\varphi \rightarrow \varphi^*$, $\pi \rightarrow \pi^*$, and $n \rightarrow \pi^*$ transitions, respectively. These bands are also observed in the spectra of the complexes with slight shifts in their frequency (Figure S5). Additionally, the spectra of all of the complexes display a medium intensity band at $\lambda \approx$ 350–362 nm (Table 4), which can be attributed to ligand-to-metal charge transfer (LMCT) from the lone pair of the pπ orbitals of the phenolate oxygen atoms to vacant d orbitals of the vanadium atoms.

Complexes **1** and **2** also show the presence of intense bands at λ = 567 and 527 nm, respectively. The VO^{3+} ion has a d^0 configuration (V^{5+}) and, therefore, no d–d transitions are expected. The high molar extinction coefficient of these bands suggests LMCT character. This is consistent with observations from other researchers, who found LMCT bands in the visible range at λ = 475–550[34] and 550–800 nm[35] in oxovanadium(V) complexes and assigned them to LMCT transitions from phenolate and alkoxide oxygen atoms to empty vanadium d orbitals. Therefore, we assign these two bands for **1** and **2** to LMCT transitions from the pπ orbitals of the phenolate and methoxy oxygen atoms to the empty d orbitals of the d^0 vanadium centers.

^{1}H NMR Spectroscopy Study

The ^{1}H NMR spectra of the ligands and complexes in [D_6]DMSO were recorded, and the relevant spectroscopic data are collected in Table 5. The ^{1}H NMR spectra of H_2L^2 (**II**) and two of its complexes (**2** and **4**) are presented in Figure 3. Two broad signals for the phenolic OH groups at δ = 10.51 (s, 1 H) and 11.44 (s, 1 H) ppm in the spectrum of **I** and at δ = 10.90 (s, 1

Table 4. UV/Vis spectroscopic data of ligands and complexes obtained in methanol.

	λ_{max} [nm] (ε, M^{-1} cm^{-1})
H_2L^1 (**I**)	309 (5.7×10^3), 270 (1.8×10^4), 205 (3.4×10^4)
H_2L^2 (**II**)	304 (1.2×10^4), 239 (3.3×10^4), 207 (4.4×10^4)
$[V^VO(\mu\text{-}L^1)(OMe)]_2$ (**1**)	567, 362 (1.4×10^3), 306 (1.4×10^4), 233 (5.0×10^4), 210 (6.0×10^4)
$[V^VO(\mu\text{-}L^2)(OMe)]_2$ (**2**)	527, 352 (2.4×10^3), 305 (2.4×10^4), 238 (6.7×10^4), 208 (9.6×10^4)
$K(H_2O)[V^VO_2(L^1)]$ (**3**)	350 (1.4×10^3), 307 (1.6×10^4), 228 (5.2×10^4), 207 (5.7×10^4)
$K(H_2O)[V^VO_2(L^2)]$ (**4**)	354 (1.4×10^3), 306 (1.4×10^4), 233 (4.9×10^4), 210 (6.0×10^4)
$Cs(H_2O)[V^VO_2(L^1)]$ (**5**)	353 (1.5×10^3), 303 (1.5×10^4), 237 (4.2×10^4), 207 (5.6×10^4)
$Cs(H_2O)[V^VO_2(L^2)]$ (**6**)	356 (1.4×10^3), 307 (1.6×10^4), 228 (5.2×10^4), 207 (5.7×10^4)

Table 5. ^{1}H NMR chemical shifts[a] [ppm] of ligands and complexes in [D_6]DMSO.

	–COOH	–OH	–OMe	Ar-H
H_2L^1 (**I**)	12.00 (s, 1 H)	10.51 (s, 1 H), 11.44 (s, 1 H)		6.91 (d, 1 H), 7.02 (m, 3 H), 7.08 (m, 2 H), 7.44 (d,1 H), 7.65 (d, 2 H), 7.85 (d, 2 H), 8.06 (d, 1 H)
$[V^VO(\mu\text{-}L^1)(OMe)]_2$ (**1**)	12.93 (s, 1 H)		4.25 (s, 3 H)	6.82 (d, 2 H), 7.36b(t, 1 H), 7.62 (m, 5 H), 7.819 (m, 3 H), 8.00 (s, 1 H)
$K(H_2O)[V^VO_2(L^1)]$ (**3**)	13.51 (s, 1 H)			6.78 (d,1 H), 6.97 (m, 4 H), 7.46 (m, 2 H), 7.83, 7.87 (m, 2 H), 8.11 (s, 1 H), 8.21 (d, 2 H)
$Cs(H_2O)[V^VO_2(L^1)]$ (**5**)	13.54 (s, 1 H)			7.04 (m, 3 H), 7.46 (m, 3 H), 7.87 (m, 3 H), 8.19 (m, 3 H)
H_2L^2 (**II**)		10.90 (s, 1 H), 10.07 (s, 1 H)		6.93 (d, 1 H), 6.99 (t, 1 H), 7.02 (m, 2 H), 7.37 (t, 1 H), 7.48 (m, 6 H), 8.04 (d, 1 H)
$[V^VO(\mu\text{-}L^2)(OMe)]_2$ (**2**)			4.25 (s, 3 H)	6.62 (m, 2 H), 6.84 (m, 4 H), 6.9 (s, 1 H), 7.5 (m, 5 H), 8.08 (s, 1 H)
$K(H_2O)[V^VO_2(L^2)]$ (**4**)				6.75 (m, 3 H), 6.95 (t, 1 H), 7.01 (m, 2 H), 7.21 (m, 3 H), 7.37 (t, 2 H), 8.04 (d, 1 H)
$Cs(H_2O)[V^VO_2(L^2)]$ (**6**)				6.68 (m, 1 H), 7.01 (t, 1 H), 7.36(d, 2 H), 7.44(d, 2 H), 7.66 (m, 5 H), 8.05 (s, 1 H)

[a] The letters given in parentheses indicate the signal multiplicity: s = singlet, d = doublet, t = triplet, and m = multiplet.

H) and 10.07 (s, 1 H) ppm in the spectrum of **II** are absent in the spectra of the complexes; therefore, the spectra confirm the coordination of the phenolate oxygen atoms to the metal ions. The signals of the aromatic protons appear in the expected region for the ligands and complexes with slight shifts in their positions. A signal due to the proton of the carboxyl group (–COOH) appears at δ = 12.00 ppm in the spectrum of **I** and at δ = 12.90–13.10 ppm in the spectra of corresponding complexes. The methyl protons of the methoxido groups of **1** and **2** resonate at δ = 4.25 ppm.

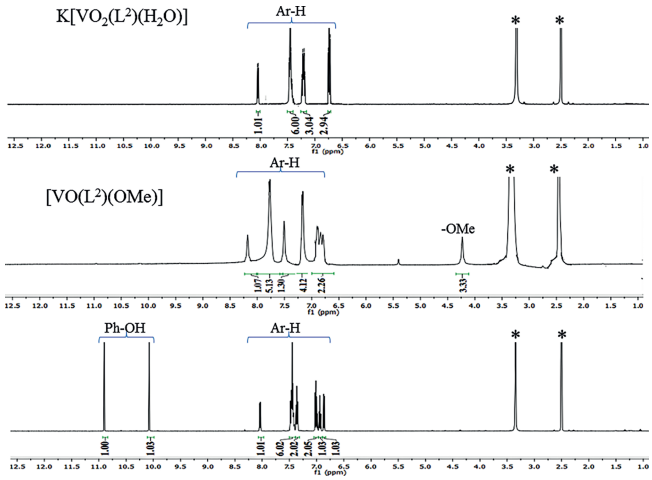

Figure 3. ^{1}H NMR spectra of ligand H_2L^2 and complexes $[VO(\mu\text{-}L^2)(OMe)]_2$ (**2**) and $K(H_2O)[V^VO_2(L^2)]$ (**4**) in [D_6]DMSO. The peaks due to solvent/H_2O have been identified by asterisks.

^{13}C NMR Spectroscopy Study

The ^{13}C NMR spectra of the ligands and complexes in [D_6]DMSO were recorded to further confirm the coordination modes of the ligands and the structures of the complexes. The relevant spectroscopic data are collected in Table 6; the ^{13}C NMR spectra of H_2L^2 and its corresponding complexes are presented in Figure S6. The chemical shifts of the carbon atoms in the vicinity of the coordinating atoms [coordination-induced shifts, see ref.[36] ($\Delta\delta$); C1/C1′, C2/C2′, and C7/C7′ in Table 6] undergo downfield shifts. The signals of the aromatic carbon atoms appear in the expected region in the spectra of the ligands and complexes with slight shifts in their positions. The signal for the carboxyl group (–COOH) appears well within the expected range in the spectra of ligands **I** and the respective complexes.

^{51}V NMR Spectral Study

Further characterization of the complexes was achieved through ^{51}V NMR spectroscopy. The chemical shifts obtained for each complex in MeOH and DMSO are listed in Table 7, and the spectra are shown in Figures S7 and S8. The spectra of the complexes derived from H_2L^1 (**1**, **3**, and **5**) in MeOH show two resonances in an approximate ratio of 30:70 at δ = –545 and –550 ppm, respectively, which probably correspond to two isomers of $[V^VO_2(L^1)(MeOH)]$. The chemical shifts are in the usual range for tridentate ONO ligands.[37] For the complexes derived from H_2L^2 in MeOH, either one (for **2**) or more species (for **4** and **6**) are detected by ^{51}V NMR spectroscopy; these species correspond to the same type of complexes as those for H_2L^1 as

Table 6. ^{13}C NMR chemical shifts [ppm] of ligands and complexes in [D_6]DMSO.

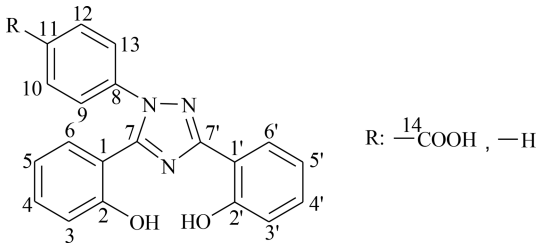

	C1/C1′	C7/C7′	C2/C2′	Other aromatic carbon atoms
H_2L^1 (**I**)	119.7	156.9	164.1	167.1, 134.3, 130.7, 130.4, 123.4, 123.0, 119.0, 117.2
$[V^VO(\mu\text{-}L^1)(OMe)]_2$ (**1**)	126.3	161.6	167.5	172.6, 134.6, 132.3, 130.8, 129.2, 128.6, 123.6, 118.9, 117.9, 114.8
($\Delta\delta$)[a]	(6.6)	(4.7)	(3.4)	
$K(H_2O)[V^VO_2(L^1)]$ (**3**)	125.3	163.2	175.5	167.3, 134.2, 129.8, 132.2, 123.4, 123.7, 120.0, 117.3
($\Delta\delta$)	(5.6)	(6.3)	(11.4)	
$Cs(H_2O)$ $[V^VO_2(L^1)]$ (**5**)	125.4	162.9	174.9	167.2, 134.3, 130.7, 126.5, 123.4, 118.7, 119.1, 117.8, 116.2, 114.6
($\Delta\delta$)	(5.71)	(6.0)	(10.8)	
H_2L^2 (**II**)	119.6	156.3	159.5	131.3, 129.2, 128.7, 126.6, 123.7, 119.2, 116.0
$[V^VO(\mu\text{-}L^2)(OMe)]_2$ (**2**)	125.7	164.7	167.5	152.5, 148.0, 145.9, 142.6, 133.4, 131.2, 130.7, 129.2, 127.1, 124.5
($\Delta\delta$)	(6.1)	(8.4)	(8.0)	
$K(H_2O)[V^VO_2(L^2)]$ (**4**)	127.4	162.6	170.2	132.3, 130.2, 129.2, 126.6, 122.8, 119.4, 117.4
($\Delta\delta$)	(7.8)	(6.3)	(10.7)	
$Cs(H_2O)[V^VO_2(L^2)]$ (**6**)	127.6	161.2	170.8	151.2, 138.1, 131.2, 128.2, 123.5, 119.4, 117.3, 116.2, 114.2
($\Delta\delta$)	(8.0)	(4.9)	(11.3)	

[a] $\Delta\delta$ = [δ(complex) – δ(free ligand)].

Table 7. ^{51}V NMR chemical shifts [ppm] of the complexes.

	MeOH (%)	DMSO (%)
1	–545 (30), –549 (70)	–493 (100)
2	–550 (100)	–456 (5), –534 (15), –568 (30), –585 (50)
3	–545 (30), –549 (70)	–469 (25), –495 (30), –519 (25), –560 (20)
4	–541 (5), –546 (5), –563 (10), –574 (80)	–447 (40), –535 (30), –565 (30)
5	–545 (10), –550 (90)	–467 (30), –559 (40), –582 (30)
6	–542 (10), –550 (20), –552 (70)	–544 (100)

well as V^V complexes with different numbers of OMe molecules, as has been observed for other V^V complexes in alcohols.[37]

In DMSO, the linewidths at half-height are much larger, and either one strong resonance (for **1** and **6**) or several are observed. The ones at $\delta \approx -550$ ppm are assigned to $[V^VO_2(L)(DMSO)]$,[38] and those at $\delta = -535$ ppm are tentatively assigned to species containing H_2O instead of DMSO in the coordination sphere. All resonances are within the expected range for VO_2 complexes with mixed O/N donor sets.[39,40]

Reactivity of the Complexes

Reactivity of Oxidovanadium(V) Complexes with H_2O_2

The reactivity of the V^VO complexes **1** and **2** in methanol with H_2O_2 was monitored by UV/Vis spectroscopy. The progressive addition of a 2×10^{-2} M H_2O_2 solution to a 1.32×10^{-4} M solution of **1** in MeOH (25 mL) caused the flattening of the LMCT band at $\lambda = 353$ nm (Figure 4, a). After the addition of a total of 1.4 mL of H_2O_2, the charge-transfer (CT) band disappeared, and the shoulders at $\lambda \approx 300$ and 280 nm developed into two bands. Additionally, the LMCT band at $\lambda = 566$ nm in the visible range also disappeared upon the dropwise addition of 3.94×10^{-2} M H_2O_2 to a 1.54×10^{-3} M solution of **1** in MeOH (25 mL; see the inset in Figure 4, a). These changes suggest the in situ generation of oxidoperoxidovanadium(V) species in solution. Similar observations were made for **2** in MeOH (see Figure 4, b).

The reactivity of the mononuclear complexes **3**, **4**, **5**, and **6** with H_2O_2 was also evaluated by UV/Vis spectroscopy, and similar changes were observed: the intensity of the charge-transfer band at $\lambda \approx 350$ nm decreased slowly (see inset of Figure 5, a and b), and a weak shoulder at $\lambda \approx 300$ nm developed upon the addition of H_2O_2 (Figure 5, a and b). Additionally, the intensity of the bands at $\lambda = 236$ and 207 nm increased. Again, these changes suggest the generation of oxidoperoxidovanadium(V) species in solution.

All these observations are consistent with the formation of oxidoperoxidovanadium(V) complexes. Usually, side-on oxidoperoxidovanadate complexes exhibit a weak absorption band ($\varepsilon \approx 10^2$–10^3 M^{-1} cm^{-1}) as the lowest-energy identifiable charge-transfer feature. In some cases, a shoulder or an additional weak peak is observable.[41]

To obtain further insights into the reactivity of the complexes towards H_2O_2, ^{51}V NMR measurements were performed (Figures S9 and S10). Upon the addition of 1 equiv. of H_2O_2 to 2 mM solutions of the complexes in MeOH, the resonances at $\delta \approx -550$ ppm decreased, and two new peaks appeared at $\delta \approx -653$ and –673 ppm. The addition of 2 equiv. of H_2O_2 led to the increase of the intensity of these two peaks, and the disappearance of the peaks assigned to the V^VO_2 complexes. For **6**, no changes were observed even after the addition of 4 equiv. of H_2O_2 (see Figure S9). The two peaks have been assigned to diperoxidovanadate(V) species.

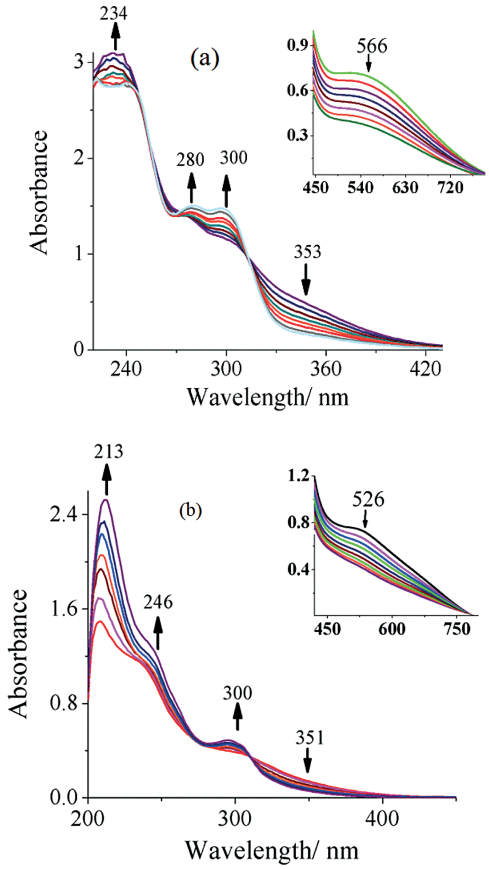

Figure 4. (a) Spectral changes observed during the reaction of **1** with H_2O_2. The spectra were recorded upon the dropwise addition of a 2×10^{-2} M H_2O_2 solution to a 1.32×10^{-4} M solution of **1** in MeOH (25 mL). The inset shows the spectral changes for the CT band of **1** during the dropwise addition of 3.94×10^{-2} M H_2O_2 to a 1.54×10^{-3} M solution of **1** in MeOH (25 mL). (b) Spectral changes observed during the titration of $[VO(\mu\text{-}L^2)(OMe)]_2$ with H_2O_2. The spectra were recorded upon the dropwise addition of 1.97×10^{-2} M H_2O_2 to a 1.06×10^{-4} M solution of **2** in MeOH. The inset shows the spectral changes for the CT band of $[VO(\mu\text{-}L^2)(OMe)]_2$ during the dropwise addition of 5.9×10^{-2} M H_2O_2 to a 2.1×10^{-3} solution of **2** in MeOH.

Evidence of the formation of a peroxidovanadate complex was found for **1** in DMSO, (see Figure 6); the addition of H_2O_2 produced a new resonance at $\delta = -564$ ppm, at the expense of the resonance at $\delta = -492$ ppm.

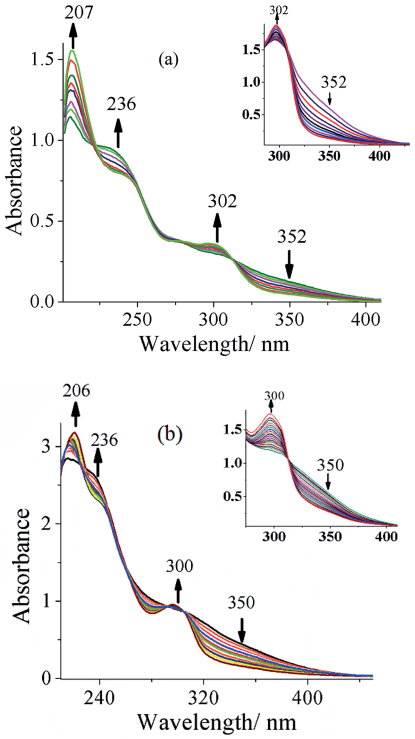

Figure 5. (a) Spectral changes observed during the reactivity of $K(H_2O)[V^{V}O_2(L^1)]$ with H_2O_2. The spectra were recorded upon the dropwise addition of 1.35×10^{-2} M H_2O_2 solution to a 1.29×10^{-3} M solution of **3** in MeOH (25 mL). The inset shows the spectral changes for the CT band of **3** during the dropwise addition of 1.40×10^{-2} M H_2O_2 to a 2.14×10^{-3} M solution of **3** in MeOH. (b) Spectral changes observed during the titration of $K(H_2O)[V^{V}O_2(L^2)]$ with H_2O_2. The spectra were recorded upon the dropwise addition of 0.7 mL of 1.47×10^{-2} M H_2O_2 to a 3.3×10^{-3} M solution of **4** in MeOH (25 mL). The inset shows the spectral changes of the CT band of **4** during the dropwise addition of 1.29×10^{-2} M H_2O_2 to a 1.76×10^{-3} M solution of **4** in MeOH (25 mL).

Catalytic Oxidative Bromination of Thymol

The oxidative bromination of thymol catalyzed by **6** in the presence of KBr, 70 % aqueous $HClO_4$, and 30 % aqueous H_2O_2 in aqueous media led to the formation of 2-bromothymol, 4-bromothymol, and 2,4-dibromothymol (Scheme 2). Among these products, 2,4-dibromothymol was found in the highest yields, possibly because of the further bromination of the monobromo product(s). The identities of the obtained products were confirmed by GC–MS and ^1H NMR spectroscopy after their separation and by comparison with literature data.[42,43]

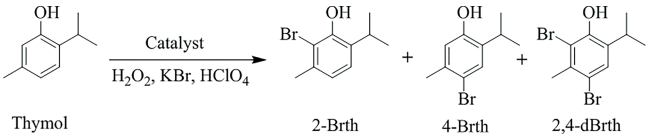

Scheme 2. Products of the oxidative bromination of thymol (2-Brth = 2-bromothymol, 4-Brth = 4-bromothymol, 2,4-dBrth = 2,4-dibromothymol).

To obtain the maximum yield of brominated products, several parameters, that is, the amount of catalyst, H_2O_2, KBr, and $HClO_4$, were varied at room temperature with **6** as a representative catalyst. Thus, for 0.010 mol (1.5 g) of thymol, three different amounts of catalyst (0.0010, 0.0020, and 0.0030 g), H_2O_2 (0.010, 0.020, and 0.030 mol), KBr (0.010, 0.020, and 0.030 mol), and $HClO_4$ (0.010, 0.020, and 0.030 mol) were added to water (20 mL), and the reactions were performed at room temperature for 2 h.

The conversion of thymol obtained in the different assays and the selectivity of the different brominated products under particular conditions are summarized in Table 8. It is clear from the data presented that the best reaction conditions to maximize the oxidative bromination (99 % conversion) of thymol are catalyst (0.0010 g), H_2O_2 (2.3 g, 0.020 mol), KBr (2.3 g,

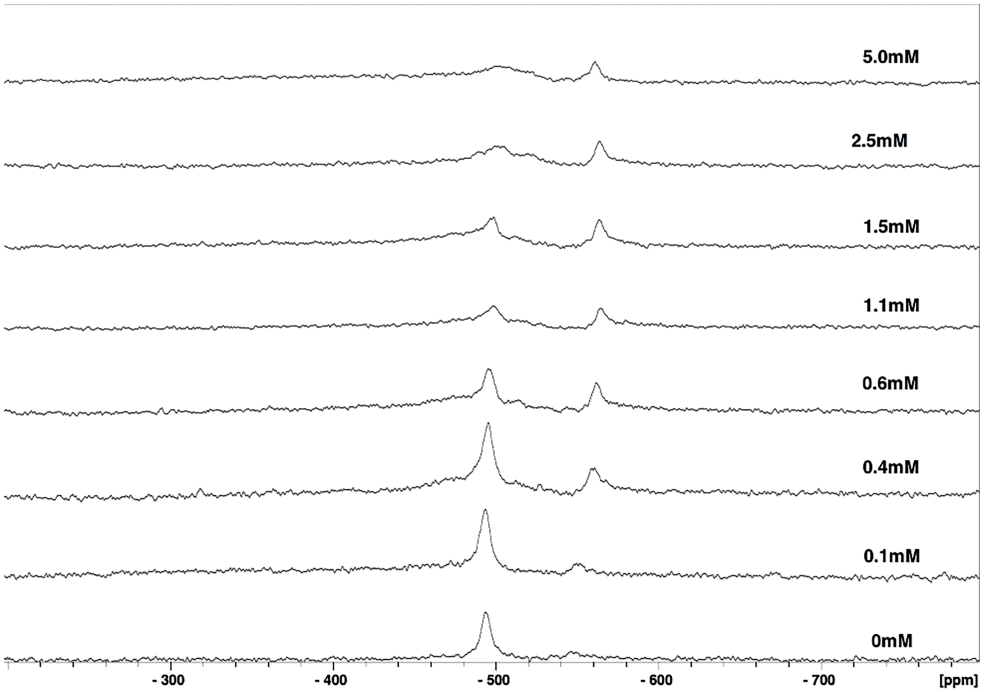

Figure 6. ^{51}V NMR spectra of solutions of **1** (2 mM) in DMSO (with 5 % D_2O) with increasing amounts of H_2O_2 (0.02 M); the concentration of H_2O_2 in each sample is indicated.

Table 8. Conversion of thymol (for 1.5 g, 0.010 mol), turnover frequency (TOF), and product selectivity with **6** as a catalyst precursor for 2 h of reaction time under different reaction conditions.

Entry	Catalyst [g (mol)]	H_2O_2 [g (mol)]	KBr [g (mol)]	$HClO_4$ [g (mol)]	Conversion [%]	TOF [h^{-1}]	2-Brth	4-Brth	2,4-dBrth
1	0.0010 (1.8×10^{-6})	1.1 (0.010)	1.2 (0.010)	1.4 (0.010)	38	950	13	85	2
2	0.0020 (3.6×10^{-6})	1.1 (0.010)	1.2 (0.010)	1.4 (0.010)	40	975	12	87	1
3	0.0030 (5.3×10^{-6})	1.1 (0.010)	1.2 (0.010)	1.4 (0.010)	41	1000	13.5	85	1
4	0.0010 (1.8×10^{-6})	2.3 (0.020)	1.2 (0.010)	1.4 (0.010)	69	1725	14	86	0
5	0.0010 (1.8×10^{-6})	3.4 (0.030)	1.2 (0.010)	1.4 (0.010)	70	1750	11	86	2
6	0.0010 (1.8×10^{-6})	2.3 (0.020)	1.2 (0.020)	2.8 (0.020)	75	1875	13	65	22
7	0.0010 (1.8×10^{-6})	2.3 (0.020)	1.2 (0.010)	4.3 (0.030)	88	2200	10.2	81	8.7
8[a]	0.0010 (1.8×10^{-6})	2.3 (0.020)	2.3 (0.020)	4.3 (0.030)	99	2475	6	21	73
9	0.0010 (1.8×10^{-6})	2.3 (0.020)	3.6 (0.030)	4.3 (0.030)	99	2475	5	7	88
10	blank	2.3 (0.020)	2.3 (0.020)	4.3 (0.030)	43		20.7	26	61

[a] Optimized reaction condition.

0.020 mol), and $HClO_4$ (4.3 g, 0.030 mol) in water (20 mL; Table 8, Entry 8). Under these conditions, the selectivity observed follows the order 2,4-dibromothymol (73 %) > 4-bromothymol (21 %) > 2-bromothymol (6 %).

The amount of catalyst does not seem to influence much the reaction outcome (see Table 8, Entries 1–3). Also, 10 mmol of $HClO_4$ is enough to obtain high conversions (Table 8, Entry 7); thus, the reaction also does not seem dependent on this reagent. On the other hand, KBr and the oxidant H_2O_2 impact the conversion and have an interesting role on the selectivity of different products. Mainly, two monobrominated products with high selectivity (up to 87 %) for 4-bromothymol are obtained at substrate/H_2O_2/KBr = 1:1:1, although the overall conversion was low. Increasing the amount of KBr improved the conversion but resulted in the formation of a considerable amount of the dibrominated product, 2,4-dibromothymol, at the expense of 4-bromothymol.

Under the optimized reaction conditions (Table 8, Entry 8), the effects of different solvent systems on the catalytic activity of **6** and the selectivity were also studied. The conversion of thymol is highest in H_2O and H_2O/MeCN (99 %), although more than 90 % conversion was obtained for all solvent systems evaluated (Table 9). The selectivity order is 2,4-dibromothymol > 4-bromothymol > 2-bromothymol.

Table 9. Solvent effects on the conversion of thymol and selectivity of products for catalyst **6**.[a]

Solvent	Conversion [%]	TOF [h^{-1}]	2-Brth	4-Brth	2,4-dBrth
Water	99	2475	6	21	73
H_2O/CH_2Cl_2	93	2325	9	17	70
$H_2O/CHCl_3$	94	2375	2	18	72
H_2O/MeOH	94	2350	4	22	73
H_2O/MeCN	99	2475	2	20	78
H_2O/hexane	91	2275	1	27	62

[a] Reaction conditions: catalyst (0.0010 g), H_2O_2 (0.020 mol, 2.3 g), KBr (0.020 mol, 2.3 g), $HClO_4$ (0.030 mol, 4.3 g).

The other complexes tested under the optimized reaction conditions showed almost the same conversion and selectivity (Table 10). A blank reaction without catalyst under the same conditions (as in Table 8, Entry 10) gave 48 % conversion. V_2O_5 under the above optimized reaction conditions resulted in 75 % conversion. Conte et al. reported 88 % conversion with NH_4VO_3 as the catalyst at NH_4VO_3/thymol/KBr/H_2O_2 ratios of 0.048:1:1:2 for 100 mM of thymol at pH 1 and 82 % conversion at NH_4VO_3/thymol/KBr/H_2O_2 ratios of 0.048:1:1:1 for 100 mM of thymol at pH 1.[42] These results suggest that the complexes are intact during the catalytic cycle; therefore, the conversion of thymol is enhanced and the selectivity of the products is altered.

Table 10. Conversion of thymol (for 1.5 g, 0.010 mol), TOF, and product selectivity for different catalysts precursors over 2 h of reaction time under the optimized reaction conditions.[a]

	Conv. [%]	TOF [h^{-1}]	2-Brth	2-Brth	2,4-dBrth
[$V^{V}O(\mu\text{-}L^1)(OMe)$] (**1**)	95	2375	16	18	65
[$V^{V}O(\mu\text{-}L^2)(OMe)$] (**2**)	94	2350	13	16	72
$K(H_2O)[V^{V}O_2(L^1)]$ (**3**)	97	2425	11	19	68
$K(H_2O)[V^{V}O_2(L^2)]$ (**4**)	96	2400	14	21	60
$Cs(H_2O)[V^{V}O_2(L^1)]$ (**5**)	99	2475	8	14	75
$Cs(H_2O)[V^{V}O_2(L^2)]$ (**6**)	98	2450	9	16	72

[a] Reaction conditions: catalyst (0.0010 g), H_2O_2 (0.020 mol, 2.3 g), KBr (0.020 mol, 2.3 g), $HClO_4$ (0.030 mol, 4.3 g), H_2O (20 mL).

The catalytic abilities of these complexes compare well with that of the vanadium complex [$V^{V}O(OMe)(MeOH)(L)$] {H_2L = 6,6′-[2-(pyridine-2-yl)ethylazanediyl]bis(methylene)bis(2,4-di-*tert*-butylphenol); the optimized reaction conditions were: substrate/H_2O_2/KBr/$HClO_4$ 1:2:2:2 for 0.010 mol of thymol}, for which 99 % conversion was obtained with 57 % selectivity towards 2,4-dibromothymol, 37 % towards 4-bromothymol, and the rest towards 2-bromothymol.[43] Dioxidomolybdenum(VI) complexes of Schiff base ligands derived from 8-formyl-7-hydroxy-4-methylcoumarin and hydrazides showed 94–99 % conversion[44] with almost the same order of selectivity for the different products.

Antiamoebic Activity

Preliminary experiments were performed to determine the in vitro antiamoebic activity of ligands H_2L^1 and H_2L^2 and their vanadium complexes against the HM1:IMSS strain of *E. histolytica* by the microdilution method. Their 50 % inhibitory concentration values (IC_{50}) are reported in Table 11 with that of the widely used antiamoebic drug metronidazole, which showed an IC_{50} of 1.8 ± 0.01 μM in our experiments. The results were estimated as the percentage of growth inhibition compared with the untreated controls and plotted as probit values as a function of the drug concentration. The IC_{50} and 95 % confidence limits were interpolated in the corresponding dose–response curves. All of the synthesized complexes showed prom-

ising antiamoebic activity with IC_{50} values in the range 0.14–1.45 μM. The data shows that both ligands have low potency to inhibit the proliferation of *E. histolytica*. However, complexation with V^V resulted in compounds with very promising activities. Among the synthesized metal complexes **1**–**6**, the highest level of activity was exhibited by **1** (IC_{50} of 0.14 ± 0.01) followed by the others in the order **4** > **5** > **2** > **6** > **3**. Thus, all metal complexes were more potent amoebicidal agents than the standard drug metronidazole (IC_{50} of 1.8 ± 0.01) and their respective ligands; therefore, the complexation to the metal center enhances the activity of the ligand. This may be explained by the Tweedy theory,[45] that is, that the chelation favors the permeation of the complexes through the lipid layer of the cell membrane.

Table 11. Antiamoebic activity of ligands and oxidovanadium(V) complexes of *N*-substituted triazole derivatives against the HM1:IMSS strain of *E. histolytica*.

	IC_{50} [μM]
I	9.38(3)
II	11.26(2)
1	0.14(1)
2	1.13(1)
3	1.45(2)
4	0.32(4)
5	0.82(1)
6	1.32(2)
MNZ	1.80(1)

Cell Viability Assay

The cytotoxicities of the compounds against human cervical cancer (HeLa) cells were accessed through a 3-(4,5-dimethylthiazol-2-yl)-2,5-diphenyltetrazolium bromide (MTT) assay.[46] As presented in Table 12, cells treated with **2**, **3**, **4**, and **6** at their IC_{50} values showed more than 90 % cell viability, whereas cells treated with **1** and **5** resulted in viability values of 89.2 and 89.6 %, respectively. Similar results were seen when the cells were treated at double their IC_{50} values. A slight increase in cell viability was usually observed if the incubation was increased from 48 to 72 h for most compounds. However, doubling of the concentration did not always result in decreased cell viability.

Table 12. Effect on cell viability of HeLa cells in response to **1**–**6** at their IC_{50} values (and double their IC_{50} values) as assessed by MTT assay.

	Concentration [μM]	48 h	72 h
1	0.14	87 ± 7	89 ± 1
1	0.28	89 ± 3	94 ± 1
2	1.13	94 ± 4	94 ± 3
2	2.26	84 ± 5	96 ± 4
3	1.45	88 ± 2	93 ± 2
3	2.90	83 ± 2	85 ± 1
4	0.32	89 ± 4	94 ± 3
4	0.64	93 ± 2	96 ± 2
5	0.82	88 ± 3	90 ± 4
5	1.64	86 ± 3	82 ± 2
6	1.32	93 ± 3	91 ± 2
6	2.64	92 ± 3	94 ± 2
MNZ	1.8	98 ± 1	96 ± 1
MNZ	3.6	99 ± 2	97 ± 2

The above results show that there is no significant reduction in cell viability of HeLa cells upon treatment with the above-mentioned compounds. Thus, these compounds are not significantly cytotoxic at the concentration necessary to have antiamoebic activity (or double of it).

Conclusions

Dinuclear oxidovanadium(V) complexes $[V^VO(\mu\text{-}L^1)(OMe)]_2$ (**1**) and $[V^VO(\mu\text{-}L^2)(OMe)]_2$ (**2**) with deferasirox {4-[3,5-bis(2-hydroxyphenyl)-1,2,4-triazol-1-yl]benzoic acid} or its unsubstituted derivative and their potassium and cesium salts of dioxidovanadium(V) analogs, that is, $K(H_2O)[V^VO_2(L^1)]$ (**3**), $K(H_2O)[V^VO_2(L^2)]$ (**4**), $Cs(H_2O)[V^VO_2(L^1)]$ (**5**), and $Cs(H_2O)[V^VO_2(L^2)]$ (**6**), have been prepared and characterized. The crystal structure of **1**·4,4′-bipyridyl (**1a**) confirmed the coordination of the ONO ligand to the vanadium ion through the nitrogen atom and the two phenolic oxygen atoms. These complexes are potential catalysts for the oxidative bromination of thymol in the presence of KBr and $HClO_4$ with H_2O_2 as the oxidant to give 2-bromothymol, 4-bromothymol, and 2,4-dibromothymol. Thus, they are considered as functional models of vanadium-dependent haloperoxidases. These complexes have also been screened against the HM1:1MSS strain of *E. histolytica*; the IC_{50} values of the metal complexes are significantly lower than that of metronidazole. These complexes are also less cytotoxic against human cervical (HeLa) cancer cell line than metronidazole; therefore, they may be promising drugs for the treatment of amoebiasis.

Experimental Section

Materials, Instrumentation, and Physical measurements: Analytical reagent-grade V_2O_5 (Loba Chemie, India), acetylacetone, hydrazine hydrate, thymol (Himedia, New Delhi), and 30 % aqueous H_2O_2, (Rankem, India) were used as received. Other chemicals and solvents were of analytical reagent grade. The ligands H_2L^1, H_2L^2,[2] and $[V^{IV}O(acac)_2]$[47] were prepared according to the methods reported previously.

The elemental analyses of the compounds were performed with an Elementar Vario-El-III instrument. The IR spectra were recorded with samples as KBr pellets with a Nicolet NEXUS Aligent 1100 series FTIR spectrometer. The electronic spectra of the ligands and complexes in MeOH were recorded with a Shimadzu 2450 UV/Vis spectrophotometer. The ^1H and ^{13}C NMR spectra of the ligands and complexes and the ^{51}V NMR spectra of the vanadium(V) complexes were recorded with a Bruker Avance III 400 MHz spectrometer with common acquisition parameters. The ^{51}V NMR spectra were recorded with the following acquisition parameters: spectral width 3960 ppm, acquisition time 39 ms, line broadening 100 Hz, dwell time 1.200, frequency 105 mHz, free induction decay (FID) resolution 13 Hz, receiver gain 2050, and number of scans > 1500. The ^{51}V NMR spectra were recorded with samples in MeOH and DMSO containing 5–10 % of deuterated solvent, and the ^{51}V chemical shifts (δ^V) are referenced to neat V^VOCl_3 as an internal standard. The chemical shifts of the ^1H and ^{13}C NMR spectra are quoted relative to tetramethylsilane (TMS) as an internal standard. The thermogravimetric analyses of the complexes were obtained under an oxygen atmosphere with a TG Stanton Redcroft STA 780 instrument. The MALDI-TOF mass spectra were measured with a Bruker Ultra-

fleXtreme-TN MALDI-TOF/TOF spectrometer with 2-(4′-hydroxybenzeneazo)benzoic acid (HABA) as the matrix. A Shimadzu 2010 plus gas chromatograph fitted with an Rtx-1 capillary column (30 m × 0.25 mm × 0.25 μm) and a flame ionization detector was used to analyze the catalytic reaction products. The identities of the products were confirmed by GC–MS with a Perkin–Elmer Clarus 500 instrument through the comparison of the fragments of each product with the available library. The percent conversion of the substrate and the selectivity of the products were calculated from the GC data by using the formulas presented elsewhere.

X-ray Crystal Structure Determination: The three-dimensional X-ray data of **1a** were collected with a Bruker Kappa Apex CCD diffractometer at 102(2) K by the ϕ-ω scan method. The reflections were measured from a hemisphere of data collected from frames that covered 0.3° in ω. A total of 32055 measured reflections were corrected for Lorentz and polarization effects and for absorption by multiscan methods based on symmetry-equivalent and repeated reflections. Of the total, 2412 independent reflections exceeded the significance level ($|F|/\sigma|F| > 4.0$. After the data collection, a multiscan absorption correction (SADABS)[48] was applied, and the structure was solved by direct methods and refined by full-matrix least-squares techniques on F^2 with the SHELX suite of programs.[49] The hydrogen atoms were included in calculated position and refined in a riding mode, except the hydrogen atom of O(5), which was located in the difference Fourier map and fixed to an oxygen atom. The refinements were performed with allowance for the thermal anisotropy of all non-hydrogen atoms. A final difference Fourier map showed no residual density in the crystal (0.687 and –0.554 e Å^{-3}). A weighting scheme $w = 1/[\sigma^2(F_o^2) + (0.112400P)^2 + 0.000000P]$ was used in the latter stages of the refinement. Further details of the crystal structure determination are given in Table 13. CCDC 1437168 (for **1a**) contains the supplementary crystallographic data for this paper. These data can be obtained free of charge from The Cambridge Crystallographic Data Centre.

Table 13. Crystal data and structure refinement details for **1a**.

	1a
Formula	$C_{54}H_{40}N_8O_{12}V_2$
Formula weight	1094.82
T [K]	102(2)
Wavelength [Å]	0.71073
Crystal system	triclinic
Space group	$P\bar{1}$
a [Å]	9.3660(18)
b [Å]	10.013(2)
c [Å]	12.987(3)
A [°]	88.059(14)
β [°]	89.482(15)
Γ [°]	89.682(16)
V [Å^3]	1217.1(4)
Z	1
F(000)	562
$D_{calcd.}$ [g cm^{-3}]	1.494
μ [mm^{-1}]	0.460
θ [°]	1.57 to 26.45
R_{int}	0.2065
Crystal size [mm^3]	0.15 × 0.08 × 0.06
Goodness-of-fit on F^2	0.971
R_1 [$I > 2\sigma(I)$] [a]	0.0787
wR_2 (all data) [b]	0.2418
Largest difference peak and hole [e Å^{-3}]	0.687 and –0.554

[a] $R_1 = \Sigma||F_o| - |F_c||/\Sigma|F_o|$. [b] $wR_2 = \{\Sigma[w(|F_o|^2 - |F_c|^2|)^2]/\Sigma[w(F_o^2)^2]\}^{1/2}$.

Catalytic Reaction – Oxidative Bromination of Thymol: The oxidative bromination of thymol was performed with the synthesized complexes as catalysts. In a typical reaction, thymol (1.5 g, 0.010 mol), 30 % aqueous H_2O_2 (2.3 g, 0.020 mol), 70 % $HClO_4$ (4.3 g, 0.030 mol), and KBr (2.3 g, 0.020 mol) were dissolved in water (20 mL) at room temperature. The catalyst (0.0010 g) was added to the reaction mixture, which was then stirred for 2 h. The obtained brominated products were analyzed quantitatively by gas chromatography, and the identities of the products were confirmed by GC–MS and ^{1}H NMR spectroscopy.

In vitro Antiamoebic Assay: All of the synthesized compounds were screened for in vitro antiamoebic activity against the HM1:IMSS strain of *E. histolytica* by the microdilution method. *E. histolytica* trophozoites were cultured in culture tubes with Diamond TYIS-33 growth medium. The tested compounds (1 mg) were dissolved in DMSO (40 μL, the level at which no inhibition of amoeba occurs).[50,51] Stock solutions (1 mg/mL) of the compounds were prepared freshly before use. Twofold serial dilutions were made in the wells of 96-well microliter plates (costar). Each test included metronidazole as a standard amoebicidal drug, control wells (culture medium plus amoebae), and a blank (culture medium only). All experiments were performed in triplicate at each concentration level and repeated three times. The amoeba suspension was prepared from a confluent culture: the medium was poured off at 37 °C, fresh medium (5 mL) was added, and the culture tube was cooled with ice to detach the organisms from the side of flask. The number of amoeba per mL was estimated with the help of a haemocytometer with trypan blue exclusion to confirm the viability. The suspension was diluted to 10^5 organisms per mL by the addition of fresh medium, and this suspension (170 μL) was added to the test and control wells in the plate so that the wells were completely filled (total volume, 340 μL). An inoculum of 1.7×10^4 organisms/well was chosen so that confluent, but not excessive growth, occurred in the control wells. The plate was sealed and gassed for 10 min with nitrogen before incubation at 37 °C for 72 h. After incubation, the growth of the amoebae in the plate was checked with a low-power microscope. The culture medium was removed through the inversion of the plate and gentle shaking. The plate was then washed immediately with sodium chloride solution (0.9 %) at 37 °C. This procedure was completed quickly, and the plate was not cooled to prevent the detachment of amoeba. The plate was allowed to dry at room temperature, and the amoebae were fixed with chilled methanol and stained with aqueous eosin (0.5 %) for 15 min after they dried. The stained plate was washed once with tap water and twice with distilled water and then allowed to dry. A portion (200 μL) of 0.1 N sodium hydroxide solution was added to each well to dissolve the protein and release the dye. The optical density of the resulting solution in each well was determined at λ = 490 nm with a microplate reader. The percentage inhibition of amoebal growth was calculated from the optical densities of the control and test wells and plotted against the logarithm of the dose of the drug tested. Linear regression analysis was used to determine the best fit line from which the IC_{50} value was found.

Cell Viability Assay: The cytotoxicity of the compounds against HeLa cells was checked through an MTT assay.[46] HeLa cells (4000 cells/well) were plated in 96-well tissue culture plates in triplicate with compounds. Each compound was added at two different concentrations: their *E. histolytica* IC_{50} value and double it. Cells treated with DMSO were used as the control. The cells were incubated for two different time periods (48 and 72 h), and the cell viability was accessed after these time intervals. The absorbance values were measured at λ = 570 nm.

$[V^VO(\mu\text{-}L^1)(OMe)]_2$ (1): A solution of H_2L^1 (0.37 g, 0.0010 mol) was prepared in hot absolute methanol (15 mL) and then filtered. A

solution of [$V^{IV}O(acac)_2$] (0.26 g, 0.0010 mol) in methanol (10 mL) was added to the above solution with stirring. After 6 h under reflux, the clear solution was reduced to 10 mL and stored in a refrigerator (ca. 5 °C). Gradually, a black solid precipitated. The solid was collected by filtration, washed with methanol and then petroleum ether (b.p. ca. 60 °C), and dried in a desiccator over silica gel, yield 0.654 g (69.7 %). $C_{44}H_{32}N_6O_{12}V_2$ (938.11): calcd. C 56.30, H 3.44, N 8.95; found C 55.9, H 3.7, N 8.9.

$[V^VO(\mu\text{-}L^2)(OMe)]_2$ (2): The black complex **2** was prepared by following the method outlined for **1** with H_2L^2 instead of H_2L^1, yield 0.613 g (72.1 %). $C_{42}H_{32}N_6O_8V_2$ (850.12): calcd. C 59.30, H 3.79, N 9.88; found C 59.3, H 3.9, N 10.0.

$K(H_2O)[V^VO_2(L^1)]$ (3): A solution of KOH (0.11 g, 0.0020 mol) in methanol (15 mL) was added slowly to a solution of **1** (0.50 g, 0.00053 mol) in methanol (150 mL) with stirring. The obtained orange solution was allowed to oxidize aerially at room temperature. After 2 d, the solution was yellow. After the solvent volume was reduced to ca. 10 mL, the solution was kept for 12 h at room temperature. The yellow solid was collected by filtration, washed with methanol, and dried in a desiccator over silica gel, yield 0.22 g (42.8 %). $C_{21}H_{15}KN_3O_7V$ (511.00): calcd. C 49.32, H 2.96, N 8.22; found C 49.0, H 3.5, N 8.1.

$K(H_2O)[V^VO_2(L^1)]$ (4): The yellow complex **4** was prepared from **2** by the procedure outlined for **3**, yield 0.24 g (51.8 %). $C_{20}H_{15}KN_3O_5V$ (467.01): calcd. C 51.39, H 3.23, N 8.99; found C 51.7, H 3.1, N 9.5.

$Cs(H_2O)[V^VO_2(L^1)]$ (5): A solution of CsOH (0.33 g, 0.0020 mol) in methanol (15 mL) was added slowly with stirring to a solution of **1** (0.50 g, 0.00053 mol) in methanol (150 mL). The obtained dark orange solution was left at room temperature for slow aerial oxidation. After 2 d, the solution became yellow. After the volume was reduced to ca. 10 mL, the solution was kept at room temperature for 12 h and a yellow solid separated. The solid was collected by filtration, washed with methanol, and dried in a desiccator over silica gel, yield 0.27 g (46.2 %). $C_{21}H_{15}CsN_3O_7V$ (604.94): calcd. C 41.68, H 2.50, N 6.94; found C 41.8, H 2.8, N 7.4.

$Cs(H_2O)[V^VO_2(L^2)]$ (6): Complex **6** was prepared similarly to **5** from **2**, yield 0.29 g (51.1 %). $C_{20}H_{15}CsN_3O_5V$ (560.95): calcd. C 42.80, H 2.69, N 7.49; found C 43.3, H 3.0, N 7.9.

Reaction of $[V^VO(\mu\text{-}L^1)(OMe)]_2$ (1) with 4,4′-Bipyridyl: Complex **1** (0.50 g, 0.00053 mol) was dissolved in methanol (50 mL), and 4,4′-bipyridyl (0.078 g, 0.00050 mol) was added. The reaction mixture was heated under reflux for 2 h with a water bath. The clear dark solution was cooled and then kept at room temperature for slow evaporation. Black crystal blocks of **1a** separated slowly within a few days. These were collected by filtration and dried under air.

Acknowledgments

M. R. M. thanks the Science and Engineering Research Board (SERB), Government of India, New Delhi for financial support of the work (EMR/2014/000529). B. S. is thankful to Indian Institute of Technology (IIT) Roorkee for awarding an MHRD fellowship. I. C. acknowledges the Portuguese Fundação para a Ciência e a Tecnologia (FCT) for an Investigador FCT contract and the IST-UTL Centers of the Portuguese NMR.

Keywords: Vanadium · Tridentate ligands · Medicinal chemistry · Antibiotics

[1] E. Nisbet-Brown, N. F. Olivieri, P. J. Giardina, R. W. Grady, E. J. Neufeld, R. Sechaud, A. J. Krebs-Brown, J. R. Anderson, D. Alberti, K. C. Sizer, D. G. Nathan, *Lancet* **2003**, *361*, 1597–1602.

[2] S. Steinhauser, U. Heinz, M. Bartholomä, T. Weyhermüller, H. Nick, K. Hegetschweiler, *Eur. J. Inorg. Chem.* **2004**, 4177–4192.

[3] a) C. R. Cornman, J. Kampf, M. S. Lah, V. L. Pecoraro, *Inorg. Chem.* **1992**, *31*, 2035–2043; b) C. R. Cornman, G. J. Colpas, J. D. Hoeschele, J. Kampf, V. L. Pecoraro, *J. Am. Chem. Soc.* **1992**, *114*, 9925–9933; c) A. D. Keramidas, S. M. Miller, O. P. Anderson, D. C. Crans, *J. Am. Chem. Soc.* **1997**, *119*, 8901–8915; d) A. Butler, *Coord. Chem. Rev.* **1999**, *187*, 17–35; e) S. Samanta, D. Ghosh, S. Mukhopadhyay, A. Endo, T. J. R. Weakley, M. Chaudhury, *Inorg. Chem.* **2003**, *42*, 1508–1517; f) S. Samanta, S. K. Dutta, M. Chaudhury, *J. Chem. Sci.* **2006**, *118*, 475–486.

[4] M. R. Maurya, A. Kumar, M. Ebel, D. Rehder, *Inorg. Chem.* **2006**, *45*, 5924–5937.

[5] a) M. R. Maurya, *J. Chem. Sci.* **2011**, *123*, 215–228; b) M. R. Maurya, A. Kumar, J. Costa Pessoa, *Coord. Chem. Rev.* **2011**, *255*, 2315–2344.

[6] V. Conte, A. Coletti, B. Floris, G. Licini, C. Zonta, *Coord. Chem. Rev.* **2011**, *255*, 2165–2177.

[7] J. A. L. da Silva, J. J. R. Fraústo da Silva, A. J. L. Pombeiro, *Coord. Chem. Rev.* **2011**, *255*, 2232–2248.

[8] a) D. C. Crans, A. D. Keramidas, S. S. Amin, O. P. Anderson, S. M. Miller, *J. Chem. Soc., Dalton Trans.* **1997**, 2799–2812; b) M. R. Maurya, C. Haldar, A. Kumar, M. L. Kuznetsov, F. Avecilla, J. Costa Pessoa, *Dalton Trans.* **2013**, *42*, 11941–11962; c) M. R. Maurya, N. Chaudhary, F. Avecilla, I. Correia, *J. Inorg. Biochem.* **2015**, *147*, 181–192; d) J. Costa Pessoa, E. Garribba, M. F. A. Santos, T. Santos-Silva, *Coord. Chem. Rev.* **2015**, *301–302*, 49–86; e) M. Sutradhar, L. M. D. R. S. Martins, M. F. C. G. da Silva, A. J. L. Pombeiro, *Coord. Chem. Rev.* **2015**, *301–302*, 200–239; f) D. C. Crans, A. Ghio, V. Conte, *J. Inorg. Biochem.* **2015**, *147*, 1–3, and other papers reported in this issue.

[9] a) A. Messerschmidt, R. Wever, *Proc. Natl. Acad. Sci. USA* **1996**, *93*, 392–396; b) M. Weyand, H. J. Hecht, M. Kiesz, M. F. Liaud, H. Vilter, D. Schomburg, *J. Mol. Biol.* **1999**, *293*, 595–611; c) M. I. Isupov, A. R. Dalby, A. Brindley, Y. Izumi, T. Tanabe, G. N. Murshudov, J. A. Littlechild, *J. Mol. Biol.* **2000**, *299*, 1035–1049; d) M. Sandy, J. N. Carter-Franklin, J. D. Martin, A. Butler, *Chem. Commun.* **2011**, *47*, 12086–12088.

[10] a) D. C. Crans, A. D. Keramidas, H. Hoover-Litty, O. P. Anderson, M. M. Miller, L. M. Lemoine, S. Pleasic-Williams, M. Vandenberg, A. J. Rossomando, L. J. Sweet, *J. Am. Chem. Soc.* **1997**, *119*, 5447–5448; b) C. Leblanc, H. Vilter, J.-B. Fournier, L. Delage, P. Potin, E. Rebuffet, G. Michel, P. L. Solari, M. C. Feiters, M. C. Leblanc, H. Vilter, J.-B. Fournier, L. Delage, P. Potin, E. Rebuffet, G. Michel, P. L. Solari, M. C. Feiters, M. Czjzek, *Coord. Chem. Rev.* **2015**, *301–302*, 134–146.

[11] a) S. S. Amin, K. Cryer, B. Zhang, S. K. Dutta, S. S. Eaton, O. P. Anderson, S. M. Miller, B. A. Reul, S. M. Brichard, D. C. Crans, *Inorg. Chem.* **2000**, *39*, 406–416; b) D. Rehder, J. Costa Pessoa, C. F. Geraldes, M. M. Castro, T. Kabanos, T. Kiss, B. Meier, G. Micera, L. Pettersson, M. Rangel, A. Salifoglou, I. Turel, D. Wang, *J. Biol. Inorg. Chem.* **2002**, *7*, 384–396; c) I. Correia, P. Adão, S. Roy, M. Wahba, C. Matos, M. R. Maurya, F. Marques, F. R. Pavan, C. Q. F. Leite, F. Avecilla, J. Costa Pessoa, *J. Inorg. Biochem.* **2014**, *141*, 83–93.

[12] a) M. R. Maurya, S. Khurana, Shailendra, A. Azam, W. Zhang, D. Rehder, *Eur. J. Inorg. Chem.* **2003**, 1966–1973; b) M. R. Maurya, A. Kumar, M. Abid, A. Azam, *Inorg. Chim. Acta* **2006**, *359*, 2439–2447; c) M. R. Maurya, S. Agarwal, M. Abid, A. Azam, C. Bader, M. Ebel, D. Rehder, *Dalton Trans.* **2006**, 937–947; d) M. R. Maurya, A. A. Khan, A. Azam, A. Kumar, S. Ranjan, N. Mondal, J. Costa Pessoa, *Eur. J. Inorg. Chem.* **2009**, 5377–5390; e) M. R. Maurya, A. A. Khan, A. Azam, S. Ranjan, N. Mondal, A. Kumar, F. Avecilla, J. Costa Pessoa, *Dalton Trans.* **2010**, *39*, 1345–1360; f) M. R. Maurya, C. Haldar, A. A. Khan, A. Azam, A. Salahuddin, A. Kumar, J. Costa Pessoa, *Eur. J. Inorg. Chem.* **2012**, 2560–2577.

[13] D. Gambino, *Coord. Chem. Rev.* **2011**, *255*, 2193–2203.

[14] a) S. A. Tengku, M. Norhayati, *Trop. Biomed.* **2011**, *28*, 194–222; b) K. Watanabe, H. Gatanaga, A. Escueta-de Cadiz, J. Tanuma, T. Nozaki, S. Oka, *PLOS Neglected Trop. Dis.* **2011**, *5*, 1318.

[15] H. Schuster, P. L. Chiodini, *Curr. Opin. Infect. Dis.* **2001**, *14*, 587–591.

[16] S. L. Stanley Jr., *Lancet* **2003**, *361*, 1025–1034.

[17] I. S. Adagu, D. Nodler, D. C. Warhurst, J. F. Rossignol, *J. Antimicrob. Chemother.* **2002**, *49*, 103–111.

[18] a) W. A. Petri, *Parasitology* **2003**, *19*, 519–526; b) F. L. En-Nahas, M. I. El-Ashmawy, *Basic Clin. Pharmacol. Toxicol.* **2004**, *94*, 226–23; c) Y. Akgun, I. H. Tacyldz, Y. Celik, *World J. Surg.* **1999**, *23*, 102–106; d) T. H. Conner, M. Stoeckel, J. Evrard, M. S. Legator, *Cancer Res.* **1977**, *37*, 629–633; e) K. Kapoor, M. Chandra, D. Nag, J. K. Paliwal, R. C. Gupta, R. C. Saxena, *Int. J. Clin. Pharmacol. Res.* **1999**, *19*, 83–88; f) H. S. Rosenkranz, W. T. Speck, *Biochem. Biophys. Res. Commun.* **1975**, *66*, 520–525; g) D. A. Rowley, R. C. Knight, I. M. Skolimowski, D. I. Edwards, *Biochem. Pharmacol.* **1980**, *29*, 2095–2098.

[19] a) H. Bayrak, A. Demirbas, N. Demirbas, S. Alpay-Karaoglu, *Eur. J. Med. Chem.* **2009**, *44*, 4362–4366; b) B. S. Holla, R. Gonsalves, S. Shenoy, *Eur. J. Med. Chem.* **2000**, *35*, 267–271; c) A. Shafiee, A. Sayadi, M. H. Roozbahani, A. Foroumadi, F. Kamal, *Arch. Pharm.* **2002**, *10*, 495–499.

[20] a) S. Papakonstantinou-Garoufalias, N. Pouli, P. Marakos, A. Chytyroglou-Ladas, *Il Farmaco* **2002**, *57*, 973–977; b) G. Turan-Zitouni, A. Kaplacikli, M. T. Z. Yildiz, P. Chevallet, D. Kaya, *Eur. J. Med. Chem.* **2005**, *40*, 607–613; c) A. R. Jalilian, S. Sattari, M. Bineshmarevasti, A. Shafiee, M. Daneshtalab, *Arch. Pharm.* **2000**, *333*, 347–354.

[21] a) L. Zahajska, V. Klimesova, J. Koci, K. Waisser, J. Kaustova, *Arch. Pharm. Pharm.* **2004**, *337*, 549–555; b) A. Foroumadi, Z. Kiani, F. Soltani, *Il. Farmaco* **2003**, *58*, 1073–107.

[22] S. M. Rabea, N. A. El-Koussi, H. Y. Hassan, T. Aboul-Fadl, *Arch. Pharm.* **2006**, *339*, 32–40.

[23] B. S. Holla, B. Veerendra, M. K. Shivananda, B. Poojary, *Eur. J. Med. Chem.* **2003**, *38*, 759–767.

[24] A. S. A. Almasirad, M. Tabatabai, A. Faizi, N. Kebriaeezadeh, A. Mehrabi, A. Dalvandi, A. Shafiee, *Bioorg. Med. Chem. Lett.* **2004**, *14*, 6057–6059.

[25] B. Chai, X. Qian, S. Cao, H. Liu, G. Song, *ARKIVOC (Gainesville, FL, U.S.)* **2003**, 141–145.

[26] A. Varvaresou, T. Siatra-Papastaikoudi, A. Tsotinis, A. Tsantili-Kakoulidou, A. Vamvakides, *Farmaco* **1998**, *53*, 320–326.

[27] A. Brucato, A. Coppola, S. Gianguzza, P. M. Provenzano, *Boll. Soc. Ital. Biol. Sper.* **1978**, *54*, 1051–1057.

[28] M. Shiroki, T. Tahara, K. Araki. Japanese Patent 75100096, **1975**; *Chem. Abstr.* 1976; 84: 59588k.

[29] a) B. Negi, K. K. Raj, S. M. Siddiqui, D. Ramachandran, A. Azam, D. S. Rawat, *ChemMedChem* **2014**, *9*, 2439–2444; b) S. M. Siddiqui, A. Salahuddin, A. Azam, *Bioorg. Med. Chem. Lett.* **2012**, *22*, 2768–2771.

[30] F. Avecilla, P. Adão, I. Correia, J. Costa Pessoa, *Pure Appl. Chem.* **2009**, *48*, 1297–1311.

[31] a) P. Adão, M. R. Maurya, U. Kumar, F. Avecilla, R. T. Henriques, M. L. Kusnetsov, J. Costa Pessoa, I. Correia, *Pure Appl. Chem.* **2009**, *81*, 1279–1296; b) I. Correia, J. Costa Pessoa, M. T. Duarte, R. T. Henriques, M. F. M. Piedade, L. F. Veiros, T. Jakusch, T. Kiss, Á. Dörnyei, M. Margarida, C. A. Castro, C. F. G. C. Geraldes, F. Avecilla, *Chem. Eur. J.* **2004**, *10*, 2301–2317.

[32] P. Adão, J. Costa Pessoa, R. T. Henriques, M. L. Kuznetsov, F. Avecilla, M. R. Maurya, U. Kumar, I. Correia, *Inorg. Chem.* **2009**, *48*, 3542–3561.

[33] M. R. Maurya, *Coord. Chem. Rev.* **2003**, *237*, 163–181.

[34] a) J. Chakravarty, S. Dutta, A. Dey, A. Chakravorty, *J. Chem. Soc., Dalton Trans.* **1994**, 557–561; b) M. J. Clague, N. L. Keder, A. Butler, *Inorg. Chem.* **1993**, *32*, 4754–4761.

[35] J. A. Bonadies, C. J. Carrano, *J. Am. Chem. Soc.* **1986**, *108*, 4088–4095.

[36] A. D. Keramidas, A. B. Papaioannou, A. Vlahos, T. A. Kabanos, G. Bonas, A. Makriyannis, C. P. Rapropoulou, A. Terzis, *Inorg. Chem.* **1996**, *35*, 357–367.

[37] D. C. Crans, H. Chen, O. P. Anderson, M. M. Miller, *J. Am. Chem. Soc.* **1993**, *115*, 6769–677.

[38] M. R. Maurya, A. Arya, U. Kumar, A. Kumar, F. Avecilla, J. Costa Pessoa, *Dalton Trans.* **2009**, 9555–9566.

[39] D. Rehder, C. Weidemann, A. Duch, W. Priebsch, *Inorg. Chem.* **1988**, *27*, 584–587.

[40] D. Rehder, *Bioinorganic Vanadium Chemistry*, John Wiley & Sons, New York, **2008**.

[41] A. B. P. Lever, H. B. Gray, *Acc. Chem. Res.* **1978**, *11*, 348–355.

[42] F. Sabuzi, E. Churakova, P. Galloni, R. Wever, F. Hollmann, B. Floris, V. Conte, *Eur. J. Inorg. Chem.* **2015**, 3519–3525.

[43] M. R. Maurya, B. Uprety, F. Avecilla, P. Adão, J. Costa Pessoa, *Dalton Trans.* **2015**, *44*, 17736–17755.

[44] M. R. Maurya, S. Dhaka, F. Avecilla, *Polyhedron* **2015**, *96*, 79–87.

[45] B. G. Tweedy, *Phytopathology* **1964**, *55*, 910–914.

[46] T. Mosmann, *J. Immunol. Methods* **1983**, *65*, 55–63.

[47] R. A. Rowe, M. M. Jones, *Inorg. Synth.* **1957**, *5*, 113–116.

[48] G. M. Sheldrick, *SADABS*, version 2.10, University of Göttingen, Germany, **2004**.

[49] G. M. Sheldrick, *Acta Crystallogr., Sect. A* **2008**, *64*, 112–122.

[50] A. T. Keene, A. Harris, J. D. Phillipson, D. C. Warhurst, *Planta Med.* **1986**, *52*, 278–284.

[51] F. D. Gillin, D. S. Reiner, M. Suffness, *Antimicrob. Agents Chemother.* **1982**, *22*, 342–345.

Received: November 17, 2015
Published Online: ■

Anticancer Complexes

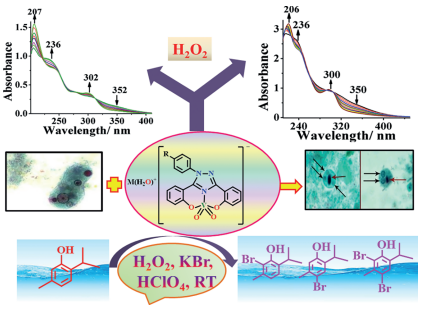

Dinuclear oxidovanadium(V) and dioxidovanadium(V) complexes of deferasirox are isolated. Their characterization, catalytic activities, and antiamoebic properties are reported.

DOI: 10.1002/ejic.201501336